TENMAK
BOREN
BOR ARAŞTIRMA ENSTİTÜSÜ

BOR DERGİSİ
JOURNAL OF BORON
https://dergipark.org.tr/boron

Characterization and oxygen reduction activities of boron-doped ordered mesoporous carbons synthesized by soft-template method

Taner Türker [1], **Çiğdem Güldür** [2,*], **Silver Güneş** [3]

[1]*Kalyon PV Solar Technologies Factory, Ankara, 06909, Türkiye*
[2]*Gazi University, Chemical Engineering Department, Ankara, 06570, Türkiye*
[3]*Gazi University, Graduate School of Natural and Applied Sciences, Ankara, 06500, Türkiye*

ARTICLE INFO

Article history:
Received February 7, 2024
Accepted July 1, 2024
Available online September 30, 2024

Research Article

DOI: 10.30728/boron.1432885

Keywords:
Boron-doping
Ordered mesoporous carbon
Oxygen reduction reaction
Soft-template synthesis

ABSTRACT

Boron-doped ordered mesoporous carbons (B-OMCs) were synthesized by a one-pot soft-templating strategy, where resorcinol and formaldehyde were used as carbon sources, boric acid was used as boron source, and Pluronic F127 was used as structure directing agent. The effect of temperature and the boric acid content on the physical and electrochemical properties of the resultant materials were investigated. Inductively coupled plasma atomic emission spectroscopy (ICP-OES) was used for elemental analysis of the samples. The synthesis temperature did not have an overall positive effect on the doping of boron with a fixed amount of boron source. However, there was a clear increase in the doped-boron content when both the temperature and the boric acid content were increased. Nitrogen adsorption analysis isotherms showed that the samples had similar ordered mesoporous structures with surface areas varying between 535 and 712 m^2/g. The uniform morphology in transmission electron microscopy (TEM) also confirmed the ordered mesoporous structure. Employing cyclic voltammetry analysis, the highest oxygen reduction activity (-0.28 mA/cm^2) was achieved with the highest boron-doping percentage (0.29%) for a synthesis temperature of 77°C and boric acid to carbon ratio of 2. These results show that the boron-doped ordered mesoporous carbon is a promising material as catalyst support for improving the oxygen reduction reaction activity.

1. Introduction

Ordered mesoporous carbons (OMCs) are promising materials for fuel cell applications, thanks to their high surface areas and electrical conductivities making them excellent candidates for catalyst support. Traditionally used electrode supports are mostly carbon blacks or their derivatives which are easy to manufacture, typically as by-products of incomplete combustion of coal or petroleum products [1]. However, they have shortcomings such as having significant microporosity. They lack a well-defined morphology which makes modeling and prediction of mass transfer and kinetics at the surface difficult. They have low electroactivity for oxygen reduction reaction and weakly bind the metallic nanoparticles [2]. On the other side, OMCs have uniform textures with pore sizes in the mesopore range, typically large enough for an effective mass transfer. At the same time, the mesostructure provides sufficient contact area for the surface reactions. The effectiveness of OMCs as catalyst support mostly depends on the morphology and the surface chemistry, which can vary significantly by the synthesis method [3,4].

There are two main strategies to synthesize OMCs, the hard-template and the soft-template methods [5]. The hard-template method involves the use of a silica-based template with a predefined ordered mesostructure. This template is infiltrated with a carbon source, followed by carbonization and removal of the template by etching. This method is successful in producing highly ordered carbon structures thanks to the ordered silica template. However, it often leads to small pore size, which is disadvantageous both for mass transfer and catalyst deposition. The use of a hard template also makes this technique costlier. The alternative strategy is the soft-templating method, which depends on the direct synthesis of mesoporous carbon in a one-step, self-assembly process. In this method, a polymerization reaction is carried out in a solvent medium, where structure-directing agents form the soft template for the polymer. The polymer is then separated and carbonized in an inert atmosphere to produce mesoporous carbon. This method provides greater flexibility and enables the synthesis of a

---

*Corresponding author: cguldur@gazi.edu.tr wider range of pore structures [6]. Depending on the synthesis parameters such as acidity, carbon-to-surfactant ratio, and carbon source type, the structure may vary in a wide range from ordered to completely disordered [7].

In recent years, heteroatom-doped ordered mesoporous carbons gained importance due to their potential for being used as metal-free electrocatalysts [8]. Many studies showed that doping of carbon surface with nitrogen, boron, phosphorus, or sulfur increases its oxygen reduction reaction (ORR) activity significantly [9-12]. This may lead to the elimination of the need to use costly noble metal catalysts, most notably platinum and palladium. The activity of doped carbons is still inferior to traditional catalysts, however, they have great potential in specific cases where high ORR activity is not needed. One example is the cathode of the microbial fuel cell, where the performance is limited by the rate of anodic reaction and the cathode cost is the primary issue rather than the activity [13].

Among different types of doped carbons, the boron-doped mesoporous carbons (B-OMCs) attracted attention due to their unique properties which make them suitable candidates as ORR catalysts. The observed oxygen reduction activity of boron-doped carbons is mainly attributed to two factors. The boron atoms adjacent to carbon atoms are positively polarized due to their lower electronegativity, therefore enhancing the adsorption of oxygen molecules. The other factor is the transfer of π-electrons in the carbon-conjugated system to the p-orbital of boron atoms, rendering them electron donors and enhancing the ORR [14]. Sheng et al. synthesized boron-doped graphene by thermal annealing in the presence of boron oxide. The resultant material showed great electroactivity toward ORR in alkaline medium, due to the electron-withdrawing capability of boron atoms [15]. Su et al. synthesized boron-doped ordered mesoporous carbons using a solvent evaporation-induced self-assembly technique and obtained high-level boron content (> 1% wt). They showed that boron-doping of carbon enhanced the ORR activity in alkaline media, and the highest activity was obtained from the sample with 1.17% boron content [16]. Zeng et al. studied boron and nitrogen co-doped ordered mesoporous carbons and their ORR activities. They reported excellent ORR activities, where the half-wave potential of the prepared catalysts shifted negatively by only 60 mV compared to the commercial Pt/C catalyst [17]. Oxygen reduction activities of some boron and other heteroatom-doped catalysts from the literature are compared in Table 1.

The electrochemical activity of B-OMCs depends on many parameters, most importantly the doped boron content and the state of boron atoms on the surface which is influenced by the synthesis conditions. The catalytic activity is generally expected to increase by the doped-boron content. Other parameters affecting the activity include the surface area and the pore size and geometry. The influence of various parameters on the physical and electrochemical properties of B-OMCs has been studied. Enterria et al. prepared hierarchical boron-doped carbons with different boron contents ranging from 0.42% to 2.37% using a combination of soft template and hydrothermal synthesis. Authors showed that the state of boron on the surface depends on the synthesis route and without the hydrothermal route the surface chemistry mostly consists of boron oxides [24]. Song et al. studied the influence of the formaldehyde-to-phenol ratio (F/P) on the boron content and pore size of B-OMCs. The surface area increased with the F/P ratio, while the boron content and the pore size first increased and then dropped off. The best results were obtained by an F/P ratio of 1.5/1 which gave ordered pore structure and a high boron content of 1.26% [25]. Zhang et al. investigated the effect of pH on pore size and the boron content. The highest boron content was reported as 1.96% (wt) at the pH of 4 [26]. These studies show that the microstructure and surface chemistry of B-OMC vary greatly by synthesis conditions. The temperature of the synthesis medium is one of the most important parameters, simultaneously affecting the soft-template structure, boric acid solubility, and the binding of boron species with the polymeric assembly. However, the effect of temperature has not been fully elucidated.

In this study, the effects of synthesis temperature and the boric acid amount on the physical and electrochemical characteristics of the resultant B-OMC materials were investigated. Materials were synthesized by a one-pot soft-templating method.

Table 1. Oxygen reduction activities of some heteroatom-doped carbon materials.

Material	Doped content (% wt)	OR peak potential (V)	OR peak current (mA or mA/cm^2)
B-doped graphene [15]	3.20	-0.34 (vs. Ag/AgCl)	-0.1 mA
N-doped carbon [18]	1.10	0.78 (vs. RHE)	-90 mA
B-doped OMC [19]	1.30	-0.28 (vs. Ag/AgCl)	-1.4 mA/cm^2
B-doped MC [20]	0.59	0.6 (vs. SCE)	unspecified
B-doped nanoparticles [21]	0.67	-0.29 (vs. Ag/AgCl)	unspecified
N-doped microspheres [22]	8.80	0.82 (vs. RHE)	-1.5 mA/cm^2
N-doped carbon black [23]	0.46	-0.19 (vs. SCE)	-0.15 mA

Characterization of the samples was carried out using ICP-OES, nitrogen adsorption, and transmission electron microscopy (TEM). Activities of selected samples towards oxygen reduction reaction were analyzed by cyclic voltammetry.

2. Experimental

2.1. Materials

Resorcinol ($C_6H_4(OH)_2$, 99%) and formaldehyde (CH_2O, 37% wt) were used as carbon sources for the polymerization reaction. Triblock copolymer Pluronic F127 (PEO-PPO-PEO, 99%) was used as a structure-directing agent. Boric acid (H_3BO_3, 99.5%) was used as a boron source, and hydrochloric acid (HCl, 37% wt) was used as a polymerization catalyst. All chemicals were purchased from Sigma Aldrich and used without further purification.

2.2. Synthesis of Boron-Doped Ordered Mesoporous Carbons

Boron-doped ordered mesoporous carbons (B-OMCs) were synthesized by the one-pot soft-template method, carried out at different temperatures and boric acid amounts to investigate their corresponding effects. In a typical synthesis, 1.25 g triblock copolymer Pluronic F127 and 1.25 g resorcinol were dissolved in 66 ml water-ethanol (1/2.3 v/v) solution. Boric acid was added to the solution, followed by magnetic stirring for 30 min. Then, 3.4 ml formaldehyde (37% wt) was added for polymerization. HCl was used as the initiator of the polymerization reaction. The synthesis mixture was stirred vigorously for another 30 min and left at rest for 4 days to allow phase separation. The same procedure was carried out at different temperatures, consisting of 17°C (ambient temperature), 37°C, 57°C and 77°C with different boric acid to carbon source ratios (w/w) in the range of 0.5 and 2.

Separation of phases was observed after four days, with the ethanol-rich phase at the top and the polymer-rich phase at the bottom. The top phase was discarded using a pipette, while the polymer-rich bottom phase was collected and washed several times. Then it was transferred to a petri dish and dried in an oven at 100°C for 24 h. The dry composite was ground and taken to pyrolysis. Pyrolysis of the composites was carried out in a tube furnace, under a controlled argon flow of 50 ml/min. Heating steps were adjusted to 180°C for 5 h, 400°C for 2 h, and 850°C for 2 h. The resultant B-OMCs were ground to fine powder before being used in characterization studies. Samples were nominated according to the formula B-OMC-t-r, where t and r stood for temperature and ratio of boric acid to carbon source (w/w), respectively. For comparison, an undoped sample was prepared with the same procedure without using boric acid and was named OMC-17-0. A schematic diagram of the synthesis is given in Fig. 1.

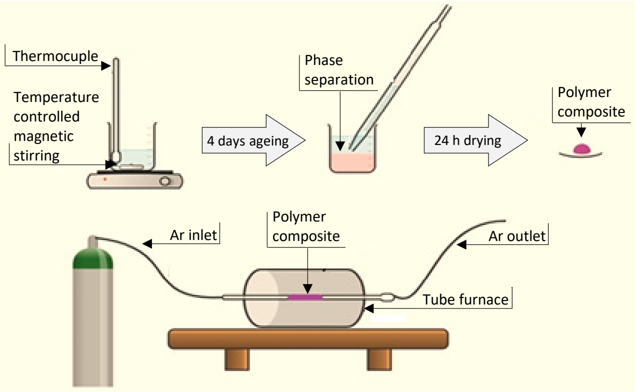

Figure 1. Schematic representation of the synthesis procedure.

2.3. Synthesis of Boron-Doped Ordered Mesoporous Carbons

2.3.1. Physical characterization

Prepared materials were subjected to physical characterization using various techniques. The surface areas, pore sizes, and structures were studied by nitrogen adsorption analysis. Measurements were carried out in a Quantachrome Instruments Autosorb model absorptiometer at 77 K. Each sample was degassed at 150°C for 2 h before the measurements. Adsorption and desorption isotherms were obtained in the relative pressure range between 0 to 1. Morphological examination of the samples was conducted by high-contrast transmission electron microscopy (TEM). Images were obtained by a FEI Tecnai G2 Spirit Biotwin model microscope operating in the range of 20-120 keV. Elemental analysis was conducted to find out the boron contents using inductively coupled plasma optic emission spectroscopy (ICP-OES). Samples were dissolved in nitric acid and hydrochloric acid and heated in a CEM Mars 6 microwave oven to 175°C for 10 min before analysis.

2.3.2. Electrochemical characterization

Oxygen reduction activities of B-OMC samples were investigated by cyclic voltammetry. Measurements were carried out using a Pine AFCBP1 potentiostat for the potential control. Voltammograms were obtained in 0.1 M KOH electrolyte with a three-electrode system, where platinum wire was used as the counter electrode and silver chloride (Ag/AgCl) was used as the reference electrode. The working electrode consisted of a glassy carbon electrode (d = 5 mm) coated with catalyst film. For the preparation of the working electrode, 10 mg of the B-OMC sample was mixed with 250 µL Nafion solution (5% wt) and homogenized mechanically to form a catalyst ink. 10 µL of this mixture was dropped on the glassy carbon surface and left to dry in ambient air for 15 min. The working electrode was polished with alumina paste between measurements. Voltammetric scans were performed in oxygen-saturated and argon-saturated electrolytes by sweeping the potential in the range between -0.2 V and 1 V (vs. Ag/AgCl) with a sweep rate of 50 mV/s until steady voltammograms were obtained.

3. Results and Discussion

B-OMC samples were synthesized at four different temperatures and four different boric acid-to-carbon source ratios (B/C). The physical and electrochemical properties of the resultant samples were characterized by various methods.

3.1. Boron-Doping Content

Boron-doping contents of the samples were determined by ICP-OES analysis and given in Fig. 2.

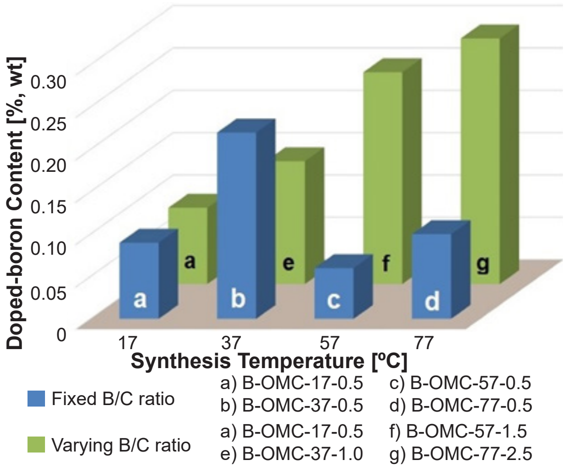

Figure 2. Boron-doping contents of samples measured by ICP-OES analysis.

When the boric acid ratio was fixed at 0.5 (w/w), increasing the temperature from 17°C to 37°C led to an increase in doped-boron content from 0.09% to 0.22% (wt%). However, at higher temperatures, there was a significant drop in the boron-doping nearly to the level obtained at room temperature. On the other side, when the boric acid ratio was increased simultaneously with temperature, the boron content showed a clear increasing trend with temperature. The highest boron content was obtained with 0.29% at 77°C using a B/C ratio of 2. Doped-boron contents can be seen in Table 2.

Table 2. BET surface areas and doped-boron contents of the samples.

Sample	sBET (m^2/g)	Doped-boron content (% wt)
OMC-17-0	684	0
B-OMC-17-0.5	702	0.09
B-OMC-37-0.5	542	0.22
B-OMC-37-1	547	0.15
B-OMC-57-0.5	538	0.06
B-OMC-57-1.5	535	0.25
B-OMC-77-0.5	712	0.10
B-OMC-77-2	617	0.29

In general, results indicate an increase in doped-boron content when both temperature and the boric acid amount are increased. This can be explained by the fact that higher concentrations of boric acid result in increased interaction of boric acid with the hydroxyl groups of the polymeric chain through hydrogen bondings. However, at the fixed boric acid ratio of 0.5 a positive linear correlation between boron-doping and temperature was not observed. Higher temperatures may also have a countering effect on boron doping, as the strength of the hydrogen bonding is known to be adversely affected by temperature [27]. Overall, it is evident that the amount of boric acid is more effective in obtaining higher boron doping. Su et al. also reported an increase in boron content with the amount of boron source [16]. Another study by Wickramaratne et al. showed similar results where the boron-doping increased with the boron source amount [28].

3.2. Surface Properties and Mesopore Structure

The nitrogen adsorption technique was used to measure the surface areas of the samples. Surface areas were calculated according to the Brunnauer-Emmet-Teller (BET) model and given in Table 2. The lowest BET surface area was measured as 535 m^2/g with OMC-57-1.5, while the highest was measured as 712 m^2/g with OMC-77-0.5. These values are comparable to commercially used carbon supports such as Vulcan XC 72 carbon black which has a surface area of 245 m^2/g [29]. Comparing the samples prepared at the same temperature, the surface areas did not vary much with the boric acid ratio or the doped boron content. An exception is the samples prepared at 77°C, where the B-OMC-77-2 sample had a significantly lower surface area than B-OMC-77-0.5. This is probably due to the growth of micelles size over a certain boric acid concentration. It has been reported that low pH values can increase the aggregation number and core radius of micelles in ethanol/water mixtures [30]. On the other side, low and high temperatures led to higher surface areas whereas mid-range temperatures gave lower surface areas, so the variation of surface area with temperature did not follow a linear correlation.

Selected samples were also examined for their adsorption and desorption isotherms to investigate the pore structure. Fig. 3 shows that the isotherms are similar and follow the type IV behavior, which is characteristic of the mesoporous materials. Significant hysteresis loops of H1 type starting around $P/P_0 = 0.4$, can be seen in all samples. The hysteresis extends to $P/P_0 = 0.8$ for OMC-77-2 and further to 0.85 for B-OMC-57-1.5 and OMC-17-0, suggesting the presence of larger pores in the latter two samples. The steepness of hysteresis is indicative of narrow pore size distribution and an ordered structure. The inset figure in Fig. 3 shows the comparison of the pore size distributions of B-OMC-77-2 and B-OMC-57-1.5. It can be seen that both materials have uniform pore sizes giving peaks at 2.7 nm and 3.7 nm for B-OMC-77-2 and B-OMC-57-1.5, respectively.

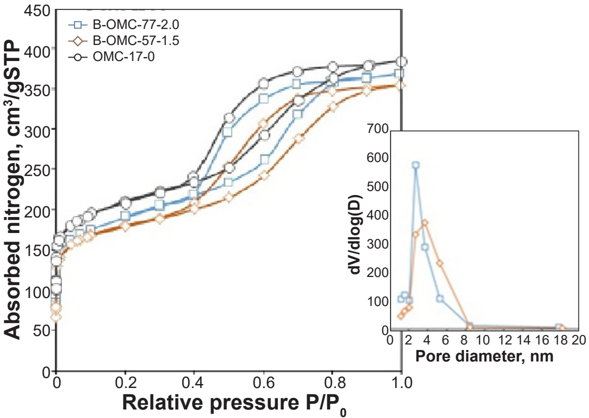

Figure 3. Adsorption-desorption isotherms of the B-OMC samples and (inset) comparison of the pore size distributions.

3.3. Transmission Electron Microscopy (TEM) Analysis

High-contrast transmission electron microscopy (TEM) images of the B-OMC-77-2 sample were taken to examine the morphology of the samples. Fig. 4 shows the images taken at different magnifications. The formation of an ordered structure is visible both in high and low magnifications. The pore texture can be defined as a three-dimensional interconnected type (*Ia3d* space group). In higher magnification (Fig. 4b), the pore sizes can be deduced to be in the mesopore range, more precisely, around 5 nm. Zhang et al. synthesized similar carbons in terms of structure and pore size [31].

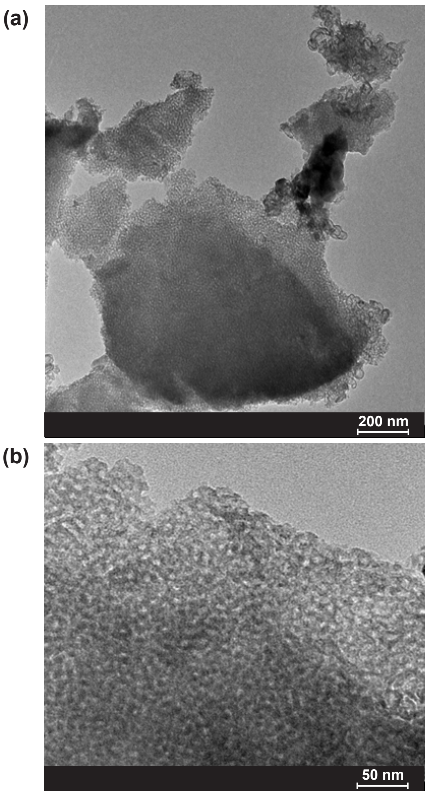

Figure 4. TEM images of the B-OMC-77-2 sample taken at (a) lower and (b) higher magnifications.

3.4. Electrochemical Activity

Cyclic voltammetry measurements were carried out to examine the oxygen reduction activities of selected samples, namely, B-OMC-77-2 and B-OMC-57-1.5 due to their relatively higher doped-boron contents. The undoped OMC-17-0 sample was also analyzed for comparison. As seen in Fig. 5(a), the OMC-17-0 sample gave a mostly featureless voltammogram, consisting of current due to reduction-oxidation on the carbon surface which is also known to be electroactive [32]. On the other hand, OMC-77-2 and OMC-57-1.5 gave apparent cathodic peaks near the potential of -300 mV which were due to the reduction of oxygen in alkaline medium. The difference between the doped and undoped samples clearly shows that boron-doping improves the electroactivity based on oxygen reduction. The peak current densities for OMC-77-2 and OMC-57-1.5 were obtained as -0.28 mA/cm^2 and -0.23 mA/cm^2 respectively, showing an increase in activity with the doped-boron content. The broad structure of peaks shows that the oxygen reduction mechanism does not occur in a single-step mechanism, but rather involves different steps and intermediates. The B-OMC-77-2 sample was also analyzed in argon-saturated electrolyte, to see the difference in activity due to the reduction of oxygen. As can be seen in Fig. 5(b), no reduction peak was observed in the Ar-saturated electrolyte, confirming that the peak is due to oxygen reduction.

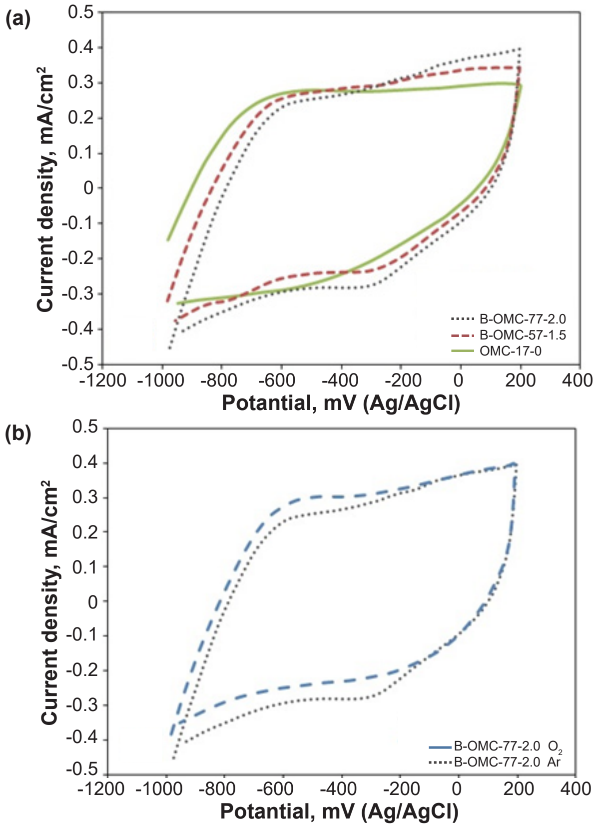

Figure 5. (a) Comparison of cyclic voltammograms of samples obtained in 0.1 M KOH electrolyte (b) Cyclic voltammograms of B-OMC-77-2 obtained in oxygen and argon saturated electrolyte.

4. Conclusions

In this study, boron-doped ordered mesoporous carbons (B-OMCs) were synthesized with a one-pot soft-templating strategy at different temperatures and boric acid-to-carbon source ratios. At a fixed boric acid ratio of 0.5, the doped boron content was generally low, and the temperature did not seem to have an overall positive effect on the doping of boron. However, the doping showed a clear increase in the boric acid amount, which can be attributed to the increased interaction of boric acid with the polymeric self-assembly. The highest doping percentage was obtained with 0.29% from the B-OMC-77-2 sample. All synthesized samples had mesoporous and orderly structures with surface areas varying between 535 and 712 m^2/g. TEM images revealed the presence of a three-dimensional mesopore texture. In the cyclic voltammograms, reduction peaks around 0.3 V showed that the B-OMC samples were electrochemically active toward oxygen reduction reaction. The peak current density increased with the doped-boron content, up to -0.28 mA/cm^2. This shows that the OR activity of carbon-supported catalysts can be further increased by means of boron doping, which may help reduce the catalyst cost in fuel cells.

Authors' contributions

All authors contributed equally to the development of this work.

References

[1] Dicks, A. L. (2006) The role of carbon in fuel cells. *Journal of Power Sources, 156*(2), 128-141. https://doi.org/10.1016/j.jpowsour.2006.02.054

[2] Chen, Y., Zhang, S., Jung, J. C. Y., & Zhang, J. (2023) Carbons as low-platinum catalyst supports and non-noble catalysts for polymer electrolyte fuel cells. *Progress in Energy and Combustion Science*, *98*, 101101. https://doi.org/10.1016/j.pecs.2023.101101

[3] Chang, H., Joo, S. H., & Pak, C. (2007) Synthesis and characterization of mesoporous carbon for fuel cell applications. *Journal of Materials Chemistry*, *17*(30), 3078. https://doi.org/10.1039/B700389G

[4] Eftekhari, A., & Fan, Z. (2017). Ordered mesoporous carbon and its applications for electrochemical energy storage and conversion. *Materials Chemistry Frontiers*, *1*(6), 1001-1027. https://doi.org/10.1039/C6QM00298F

[5] Liang, C., Li, Z., & Dai, S. (2008) Mesoporous carbon materials: Synthesis and modification. *Angewandte Chemie-International Edition*, *47*(20), 3696-3717. https://doi.org/10.1002/anie.200702046

[6] Chauhan, S. (2021) Synthesis of ordered mesoporous carbon by soft template method. *Materials Today: Proceedings*, *81*, 842-847. https://doi.org/10.1016/j.matpr.2021.04.257

[7] Ma, T.-Y., Liu, L., & Yuan, Z. Y. (2013) Direct synthesis of ordered mesoporous carbons. *Chemical Society Reviews*, *42*(9), 3977-4003. https://doi.org/10.1039/C2CS35301F

[8] Gao Y., Wang, Q., Ji, G., Li, A., & Niu, J. (2021) Doping strategy, properties and application of heteroatom-doped ordered mesoporous carbon. *RSC Advances*, *11*, 5361-5383. https://doi.org/10.1039/D0RA08993A

[9] Ozaki, J.-I., Kimura, N., Anahara, T., & Oya, A. (2007) Preparation and oxygen reduction activity of BN-doped carbons. *Carbon*, *45*(9), 1847-1853. https://doi.org/10.1016/j.carbon.2007.04.031

[10] Paraknowitsch, J. P., & Thomas, A. (2013). Doping carbons beyond nitrogen: an overview of advanced heteroatom doped carbons with boron, sulfur, and phosphorus for energy applications. *Energy & Environmental Science*, *6*(10), 2839. https://doi.org/10.1039/C3EE41444B

[11] Yang, T., Liu, J., Zhou, R., Chen, Z., Xu, H., Qiao, S. Z., & Monteiro, M. J. (2014) N-doped mesoporous carbon spheres as the oxygen reduction reaction catalysts. *Journal of Materials Chemistry A*, *2*(42), 18139-18146. https://doi.org/10.1039/C4TA04301D

[12] Xie, L., Zhou, W., Qu, Z., Ding, Y., Gao, J., Sun, F., Qin, Y. (2022) Understanding the activity origin of oxygen-doped carbon materials in catalyzing the two-electron oxygen reduction reaction towards hydrogen peroxide generation. *Journal of Colloid and Interface Science*, *610*, 934-943. https://doi.org/10.1016/j.jcis.2021.11.144

[13] Zhang, P., Liu, X. H., Li, K. X., & Lu, Y. R. (2015) Heteroatom-doped highly porous carbon derived from petroleum coke as efficient cathode catalyst for microbial fuel cells. *International Journal of Hydrogen Energy*, *40*(39): 13530-13537. https://doi.org/10.1016/j.ijhydene.2015.08.025

[14] Yang, L., Jiang, S., Zhao, Y., Zhu, L., Chen, S., Wang, X., & Hu, Z. (2011) Boron-doped carbon nanotubes as metal-free electrocatalysts for the oxygen reduction reaction. *Angewandte Chemie, International Edition*, *50*(31), 7132-7135. https://doi.org/10.1002/anie.201101287

[15] Sheng, Z. H., Gao, H. L., Bao, W. J., Wang, F. B., Xia, X. H. (2012). Synthesis of boron-doped graphene for oxygen reduction reaction in fuel cells. *Journal of Materials Chemistry*, *22*, 390. https://doi.org/10.1039/C1JM14694G

[16] Su, J., Cao, X., Wu, J., Jin, C., Tian, J. H., & Yang, R. (2016). One-pot synthesis of boron-doped ordered mesoporous carbons as efficient electrocatalysts for oxygen reduction reaction. *RSC Advances*, *6*, 24728-24737. https://doi.org/10.1039/C6RA01296E

[17] Zeng, K., Su J., Cao, X., Zheng, X., Li, X., Tian, J.-T., & Yang, R. (2020) B, N Co-Doped ordered mesoporous carbon with enhanced electrocatalytic activity for the oxygen reduction reaction. *Journal of Alloys and Compounds*, *824*, 153908. https://doi.org/10.1016/j.jallcom.2020.153908

[18] Barrera, D., Florent, M., Sapag, K., & Bandosz, T. J. (2019) Insight into the mechanism of oxygen reduction reaction on micro/mesoporous carbons: Ultramicropores versus nitrogen-containing catalytic centers in ordered pore structure. *ACS Applied Energy*

Materials, *2*(10), 7412-7424. https://doi.org/10.1021/acsaem.9b01427

[19] Bo, X., & Guo, L. (2013) Ordered mesoporous boron-doped carbons as metal-free electrocatalysts for the oxygen reduction reaction in an alkaline solution. *Physical Chemistry Chemical Physics*, *15*, 2459-2465. https://doi.org/10.1039/c2cp43541a

[20] Li, J., Shi, J., Bao, A., & Jia, J. (2021) Development of boron-doped mesoporous carbon materials for use in CO2 capture and electrochemical generation of H2O2. *ACS Omega*, *6*(12), 8438-8446. https://doi.org/10.1021/acsomega.1c00197

[21] Panomsuwan, G., Saito, N., & Ishizaki, T. (2015) Electrocatalytic oxygen reduction activity of boron-doped carbon nanoparticles synthesized via solution plasma process. *Electrochemistry Communications*, *59*, 81-85. http://doi.org/10.1016/j.elecom.2015.07.005

[22] Ferrero, G. A., Preuss, K., Fuertes, A. B., Sevilla, M., & Titirici, M. M. (2016) The influence of pore size distribution on the oxygen reduction reaction performance in nitrogen-doped carbon microspheres, *Journal of Materials Chemistry A*, *4*, 2581-2589. http://doi.org/10.1039/C5TA10063A

[23] Zahoor, A., Christy, M., Hwang, Y. J., Lim, Y. R., Kim, P., & Nahm, K. S. (2014) Improved electrocatalytic activity of carbon materials by nitrogen doping, *Applied Catalysis B: Environmental*, *147*, 633-641. https://doi.org/10.1016/j.apcatb.2013.09.043

[24] Enterria, M., Pereira, M. F. R., Martins, J. I., & Figueiredo, J. L. (2015). Hydrothermal functionalization of ordered mesoporous carbons: the effect of boron on supercapacitor performance. *Carbon*, *95*, 72-83. https://doi.org/10.1016/j.carbon.2015.08.009

[25] Song, J., Zhang, Y., & Liu, Y. (2015). The influence of formaldehyde/phenol molar ratio on the microstructure of B-OMCs. *RSC Advances*, *5*(27), 20734-20740. https://doi.org/10.1039/C4RA13078B

[26] Zhang, Y., Dai, W., Liu, Y., Ma, B. (2017). Synthesis and characterization of boron-doped ordered mesoporous carbon by evaporation-induced self-assembly under HCl conditions. *RSC Advances*, *7*(14), 8250–8257. https://doi.org/10.1039/C6RA26841B

[27] Ohtaki, H. (2003). Effects of temperature and pressure on hydrogen bonds in water and formamide. *Journal of Molecular Liquids*, *103-104*, 3-13. https://doi.org/10.1016/S0167-7322(02)00124-1

[28] Wickramaratne, N., & Jaroniec, M. (2012). Adsorption and structural properties of ordered mesoporous carbons synthesized by soft-templating in the presence of boric acid and tetraethyl orthosilicate. *RSC Advances*, *2*(5), 1877. https://doi.org/10.1039/C2RA00920J

[29] Pantea, D., Darmstadt, H., Kaliaguine, S., & Roy C. (2003) Electrical conductivity of conductive carbon blacks: Influence of surface chemistry and topology. *Applied Surface Science*, *217*(1-4):181-193. https://doi.org/10.1016/S0169-4332(03)00550-6

[30] Alexander, S., de Vos, W. M., Castle, T. C., Cosgrove, T., & Prescott, S. W. (2012) Growth and shrinkage of pluronic micelles by uptake and release of flurbiprofen: Variation of pH. *Langmuir*, *28*(16), 6539-6545. https://doi.org/10.1021/la204262w

[31] Zhang, C., Wang, G., Zhang, X., & Zhang, Y. (2016). High-loading Pt nanoparticles on mesoporous carbon with large mesopores for highly active methanol electro-oxidation. *Journal of Solid-State Electrochemistry*, *20*(6), 1705-1712. https://doi.org/10.1007/s10008-016-3177-8

[32] Ma, Y., Wang, H., Ji, S., Goh, J., Feng, H., & Wang, R. (2014) Highly active Vulcan carbon composite for oxygen reduction reaction in alkaline medium. *Electrochimica Acta*, *133*, 391-398. https://doi.org/10.1016/j.electacta.2014.04.080